ARTICLE OPEN

Check for updates

Functional inactivation of pulmonary MAIT cells following 5-OP-RU treatment of non-human primates

Shunsuke Sakai[1], Nickiana E. Lora[1], Keith D. Kauffman[1], Danielle E. Dorosky[1], Sangmi Oh[2], Sivaranjani Namasivayam[3], Felipe Gomez[4], Joel D. Fleegle[4], Tuberculosis Imaging Program*, Cecilia S. Lindestam Arlehamn[6], Alessandro Sette[6,7], Alan Sher[3], Gordon J. Freeman[8], Laura E. Via[2,4,5], Clifton E. Barry III[2,5] and Daniel L. Barber[1]✉

Targeting MAIT cells holds promise for the treatment of different diseases and infections. We previously showed that treatment of *Mycobacterium tuberculosis* infected mice with 5-OP-RU, a major antigen for MAIT cells, expands MAIT cells and enhances bacterial control. Here we treated *M. tuberculosis* infected rhesus macaques with 5-OP-RU intratracheally but found no clinical or microbiological benefit. In fact, after 5-OP-RU treatment MAIT cells did not expand, but rather upregulated PD-1 and lost the ability to produce multiple cytokines, a phenotype resembling T cell exhaustion. Furthermore, we show that vaccination of uninfected macaques with 5-OP-RU+CpG instillation into the lungs also drives MAIT cell dysfunction, and PD-1 blockade during vaccination partly prevents the loss of MAIT cell function without facilitating their expansion. Thus, in rhesus macaques MAIT cells are prone to the loss of effector functions rather than expansion after TCR stimulation in vivo, representing a significant barrier to therapeutically targeting these cells.

Mucosal Immunology (2021) 14:1055–1066; https://doi.org/10.1038/s41385-021-00425-3

INTRODUCTION

Mucosal Associated Invariant T (MAIT) cells are restricted by the nonpolymorphic MHC class I-like molecule MR1 and express TCRs specific for small molecule metabolites produced by microbes.[1,2] 5-OP-RU, a derivative of intermediates produced during bacterial riboflavin biosynthesis, is a major MR1 ligand that is recognized by a majority of MR1-restricted T cells.[3–5] MAIT cells display pro-inflammatory, cytotoxic, and tissue-repair properties.[6–8] Given the non-polymorphic nature of MR1 there is interest in targeting MAIT cells through vaccination or as therapies for the treatment of various conditions including cancer and infections. Indeed, using mouse models, MAIT cells have been shown to be important for the control of certain bacterial infections,[9–11] and they can easily be driven to expand to large numbers in vivo via vaccination with antigen and adjuvant.[7,12]

Targeting MAIT cells may be useful during *Mycobacterium tuberculosis* (Mtb) infection.[13] Recently, it was shown that MR1 deficient mice have no defect in bacterial control or survival after Mtb infection,[14,15] and the presence of large populations of MAIT cells at the time of Mtb exposure has no impact on host resistance.[14–16] Therefore, the murine model data indicate that pre-infection vaccination of MAIT cells may not be beneficial for Mtb infection. However, we showed that treatment of mice harboring a chronic Mtb infection with 5-OP-RU was able to reduce bacterial loads ~10 fold in 3 weeks in a manner dependent on IL-17A,[14] indicating that post-exposure stimulation of MAIT cells may be a promising host directed therapy for tuberculosis (TB). While there is significant overlap in the gene expression patterns of human and mouse MAIT cells[7], there are several key differences between murine and non-human primate (NHP)/human MAIT cells. For example, the majority of mouse MAIT cells are $CD4^{-}CD8^{-}$ IL-17A-producing MAIT17 cells, while most human and macaque MAIT cells are $CD8^{+}$ IFN-γ-producing MAIT1 cells.[8,17–19] Moreover, mice have several limitations in their ability to model human TB. In contrast, Mtb infection of macaques recapitulates most features of human TB, and macaques are considered the gold standard pre-clinical model of TB.[20] Therefore, we tested the potential therapeutic efficacy of 5-OP-RU instillation into the lungs of Mtb infected rhesus macaques.

In contrast to mice, there was no therapeutic benefit observed with 5-OP-RU treatment of macaques with TB. MAIT cells in these animals failed to expand, upregulated high levels of PD-1 and became functionally impaired. To ask if the loss of function was due to Mtb infection or PD-1, we vaccinated macaques with 5-OP-RU+CpG instillation in the lungs in the presence or absence of PD-1 blocking antibody and examined MAIT cell expansion and function. Again, MAIT cells failed to expand and lost the ability to produce cytokines. PD-1 blockade during 5-OP-RU + CpG vaccination did not result in MAIT cell expansion but partly alleviated the loss of cytokine producing ability. This study provides insight into

[1]T Lymphocyte Biology Section, Laboratory of Parasitic Diseases, National Institute of Allergy and Infectious Diseases, Bethesda, MD, USA. [2]Tuberculosis Research Section, Laboratory of Clinical Immunology and Microbiology, National Institute of Allergy and Infectious Diseases, Bethesda, MD, USA. [3]Immunobiology Section, Laboratory of Parasitic Diseases, National Institute of Allergy and Infectious Diseases, Bethesda, MD, USA. [4]Division of Intramural Research, National Institute of Allergy and Infectious Diseases, National Institutes of Health, Bethesda, MD, USA. [5]Institute of Infectious Disease and Molecular Medicine, University of Cape Town, Cape Town, South Africa. [6]Center for Infectious Disease, La Jolla Institute for Immunology, La Jolla, CA, USA. [7]Department of Medicine, University of California San Diego, La Jolla, CA, USA. [8]Department of Medical Oncology, Dana-Farber Cancer Institute, Harvard Medical School, Boston, MA, USA. *A list of authors and their affiliations appears at the end of the paper. ✉email: barberd@niaid.nih.gov

Received: 24 March 2021 Revised: 28 May 2021 Accepted: 6 June 2021
Published online: 22 June 2021

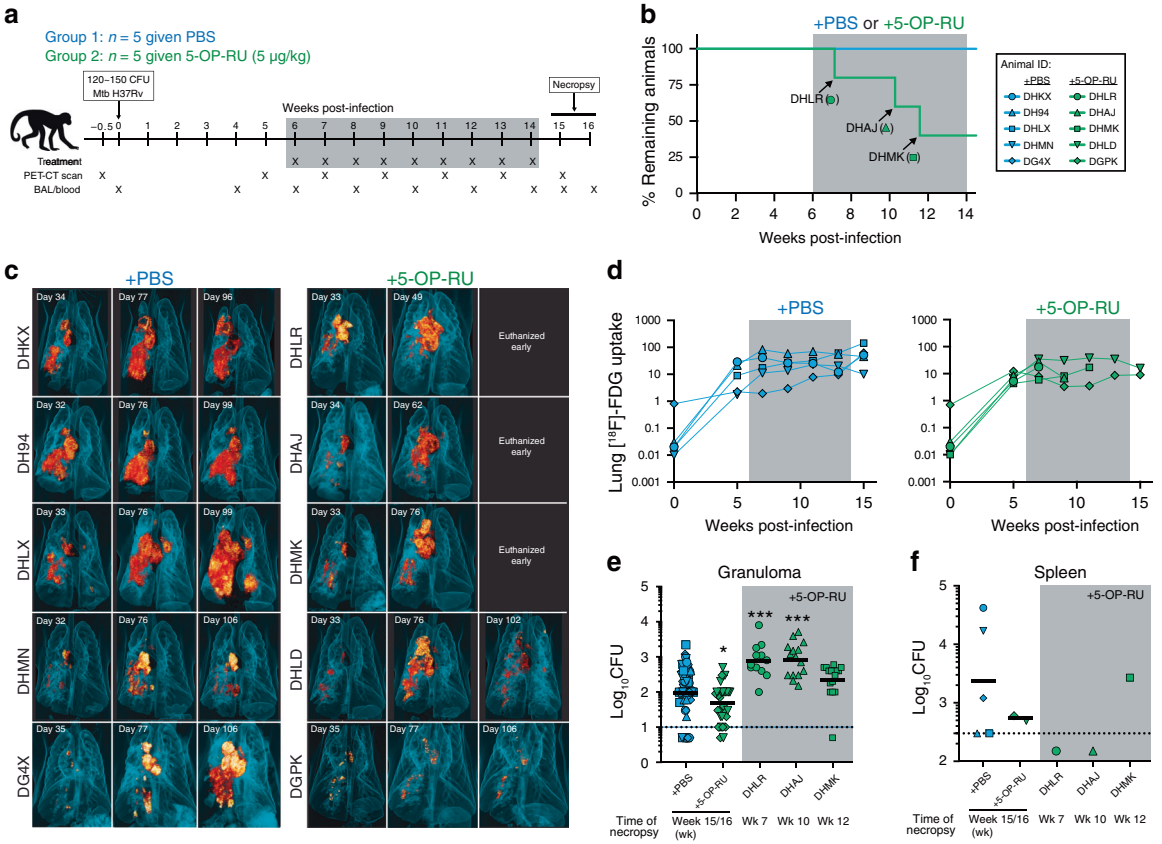

Fig. 1 5-OP-RU treatment in Mtb-infected macaques does not enhance control of the infection. a Ten animals were infected with 120-150 colony forming units (CFU) of Mtb H37Rv. Starting 6 weeks post-infection, animals were intratracheally treated with PBS ($n = 5$) or 5-OP-RU ($n = 5$). Animals were necropsied at weeks 15 or 16 post-infection. **b** Percentage of remaining animals in the 2 groups were plotted against the weeks after Mtb infection. Three 5-OP-RU treated animals (DHLR, DHAJ, DHMK) were humanly euthanized early due to the development of severe pulmonary distress. **c** Three-dimensional volume renderings of PET/CT scans of each animal at week 5 and 11 post-infection and at necropsy. **d** The lung total [^{18}F]-FDG uptake (total lesion glycolysis, TLG) value in PBS (left) and 5-OP-RU treated (*right*) animals. Bacterial loads in the granulomas (**e**) and spleens (**f**) shown in pooled animals by experimental group and individual animals euthanized early. Each symbol represents an individual tissue sample from indicated animal. Dotted line indicates limit of detection. *$p < 0.05$, ***$p < 0.001$.

basic in vivo MAIT cell biology in NHPs and identifies a major barrier to the translatability of MAIT cell directed therapies. Unlike mice, administration of 5-OP-RU during infection or with adjuvant in macaques fails to expand MAIT cells and instead leads to MAIT cell dysfunction. Strategies to drive MAIT cell expansion in macaques are needed to test their therapeutic potential during TB and other diseases.

RESULTS

5-OP-RU treatment in Mtb-infected macaques does not enhance control of the infection

To examine the therapeutic efficacy of MAIT cell stimulation during Mtb infection, macaques were treated intratracheally with PBS or 5-OP-RU from week 6 to week 14 post-infection (Fig. 1a). Necropsies were planned for week 15-16. All five PBS treated control animals survived until the pre-determined endpoint. In contrast, three of the five 5-OP-RU treated animals developed acute signs of disease (cough and labored breathing) and were humanly euthanized early (Fig. 1b). All animals in both groups had relatively stable lung disease as measured by [^{18}F]-FDG-PET/CT imaging of the lungs (Fig. 1c, d). Upon necropsy, bacterial loads in individually resected granulomas were measured. Granulomas from PBS and 5-OP-RU treated macaques had similar overall numbers of bacteria (Fig. 1e). However, when control animals were compared to just the two 5-OP-RU treated macaques which remained until the week15/16 pre-determined endpoint, there was a slight decrease in the numbers of bacteria in treated animals (Fig. 1e). Two of the 5-OP-RU treated macaques that were euthanized early (DHLR at week 7 and DHAJ at week 10) displayed slightly increased bacterial loads in the granulomas, but we could not distinguish whether the increase in the number of bacteria was due to the earlier necropsy or 5-OP-RU treatment (Fig. 1e). Moreover, there was no significant difference in the number of bacteria in the spleens of both groups (Fig. 1f).

Since three of the 5-OP-RU treated macaques (DHLR, DHAJ, DHMK) had acute clinical signs after treatment, we assessed the levels of airway constriction in the animals by measuring the maximum diameter of bronchi on CT images collected at baseline and during Mtb infection. The three 5-OP-RU treated animals that were euthanized early each showed rapid reductions in airway diameter after treatment relative to the PBS control treated animals and the two other 5-OP-RU treated animals that did not develop severe signs of distress (Fig. 2a, b, S2). The bronchoconstriction was not associated with either higher bacterial loads in the pulmonary lymph nodes (LNs) (Fig. 2c) or overall LN [^{18}F]-FDG uptake on PET/CT scans (Figs. 1c and 2d). However, a trend was observed in which animals with bronchoconstriction had at least one very cellular pulmonary LN at necropsy relative to the 5-OP-RU treated animals that did not develop respiratory distress or the PBS treated animals (Fig. 2e). On visual inspection at necropsy, it was apparent that the enlarged LNs were impinging on the bronchus. Therefore, it seems likely that lymphadenopathy-associated airway constriction and not expansive tubercular lung

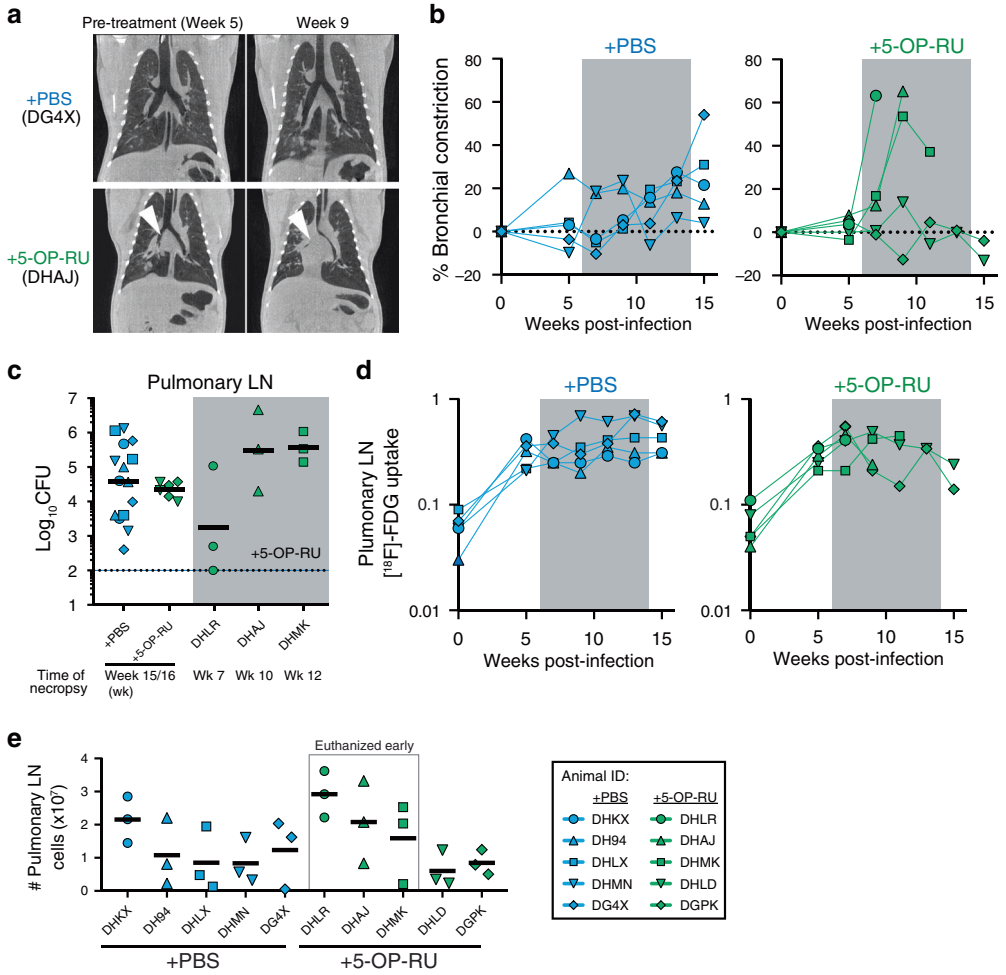

Fig. 2 Early necropsies of 5-OP-RU treated animals were associated with bronchoconstriction. a Example chest CT images from PBS (top) and 5-OP-RU (bottom) treated animals chosen to illustrate the bronchial constriction (shown by the arrowheads). **b** Percent change of airway constriction of PBS (left) and 5-OP-RU treated (right) animals. Airway constriction was determined by comparing the diameter of bronchi at baseline and after infection. **c** Bacterial loads in the pulmonary LNs shown in pooled animals by experimental group and individual animals euthanized early. Each symbol represents an individual tissue sample from indicated animal. Dotted line indicates limit of detection. **d** The lung total [^{18}F]-FDG uptake (total lesion glycolysis, TLG) value in PBS (left) and 5-OP-RU treated (right) animals. **e** Number of total viable cells within pulmonary LNs. Each symbol represents an individual tissue from indicated animal.

lesions was responsible for the acute clinical signs that led to the early euthanasia of these three macaques treated with 5-OP-RU. Rhesus macaques have been shown previously to be particularly susceptible to lethal LN pathology[21,22], so it is not clear if the 5-OP-RU treatment was the direct cause of the bronchoconstriction. Regardless, 5-OP-RU treatment during Mtb infection did not have a clinical or microbiological benefit in rhesus macaques.

MAIT cells become activated but do not expand after 5-OP-RU instillation

We next measured the frequency of MAIT cells in the bronchoalveolar lavage (BAL) and peripheral blood using rhesus macaque MR1/5-OP-RU tetramers. Consistent with the previous findings,[23] the frequency of MAIT cells in the airway and blood did not change in the PBS treated group after Mtb infection (Fig. 3a–d). In contrast to previous reports in the mouse model showing large increases in MAIT cells after 5-OP-RU administration,[14,15] 5-OP-RU treatment in the infected macaques did not result in the expansion of airway or circulating MAIT cells (Fig. 3a–d). To examine whether MAIT cells entered cell cycle, we measured Ki-67 expression in MAIT cells isolated from the BAL and blood. While there was a small increase in the Ki-67 expression by MAIT cells in the BAL at 4 weeks post-infection, we did not observe clear differences in their Ki-67 expression between PBS and 5-OP-RU treated groups during treatment (Fig. 3e–g). In contrast to the BAL, MAIT cells in the blood significantly upregulated Ki-67 at 4 weeks post-infection in both groups (Fig. 3g). After week 4 the levels of Ki-67 expression in blood borne MAIT cells then decreased back toward baseline, but after 5-OP-RU treatment was started on week 6 there was a clear increase in Ki-67^{+} MAIT cells (Fig. 3g).

PD-1 is induced by TCR signaling, so we next examined its expression to ask if MAIT cells were stimulated through their TCR after 5-OP-RU treatment. While PD-1 expression by MAIT cells was not changed in the BAL or blood of control animals, 5-OP-RU treatment led to a striking upregulation of PD-1 by MAIT cells in both compartments (Fig. 3h–j), indicating that MAIT cells clearly received antigen stimulation through their TCRs after 5-OP-RU treatment. At necropsy, we examined multiple tissue sites to ask if MAIT cells expanded in any tissue. There was no impact of 5-OP-RU administration on the frequency of MAIT cells in the thymus, spleen, pulmonary LNs, granulomas or instillation site lesions (Fig. 3k). Overall, these data demonstrate that 5-OP-RU treatment in Mtb infected rhesus macaques indeed activates MAIT cells via TCR stimulation leading to Ki67 and PD-1 expression but fails to induce their expansion.

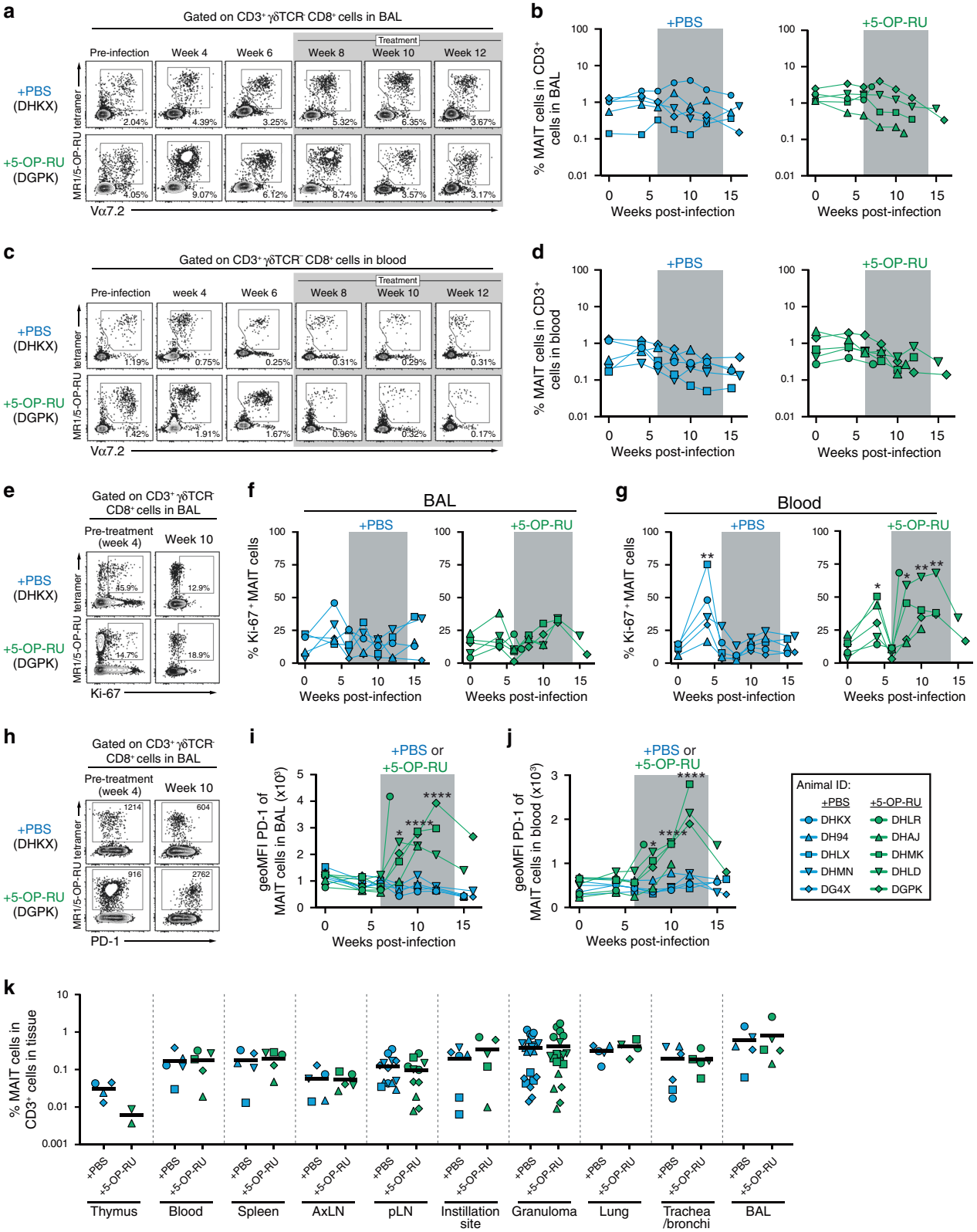

Fig. 3 MAIT cells become activated but do not expand after 5-OP-RU instillation. a Example FACS plots of MR1/5-OP-RU tetramer staining of cells in the bronchoalveolar lavage (BAL). **b** Kinetics of the frequency of MAIT cells among $CD3^+$ cells in the airway. **c** Example FACS plots of MR1/5-OP-RU tetramer staining of cells in the blood. **d** Kinetics of the frequency of MAIT cells among $CD3^+$ cells in the blood. **e** Example FACS plots of Ki-67 expression on MAIT cells in the BAL from week 4 and 10 post-infection. Summary graphs showing the percentage of $Ki\text{-}67^+$ MAIT cells in the BAL (**f**) or blood (**g**). **h** Example FACS plots of PD-1 expression on MAIT cells in the BAL from week 4 and 10 post-infection. Summary graphs showing the geometric mean fluorescent intensity (geoMFI) of PD-1 on MAIT cells in the BAL (**i**) or blood (**J**). **K** Percentage of MAIT cells in the indicated tissues at necropsy. Each symbol represents an individual tissue sample from indicated animal. $^*p < 0.05$, $^{**}p < 0.01$, $^{****}p < 0.0001$ as compared to the pre-infection time point.

5-OP-RU treatment leads to MAIT cell dysfunction in Mtb infected macaques

We next evaluated the impact of 5-OP-RU treatment on the function of MAIT cells. Cells from the BAL or blood were stimulated with 5-OP-RU or PMA/ionomycin, and production of IFN-γ, TNF-α, IL-17A and GM-CSF was measured by intracellular cytokine staining (Fig. 4a). The vast majority of MAIT cells in both blood and BAL produced cytokines after stimulation with PMA/ionomycin (Fig. 4b–d). However, prior to instillation of 5-OP-RU, there were major differences in the responses of BAL vs blood MAIT cells after in vitro 5-OP-RU stimulation. Approximately 75% of MAIT cells in the BAL produced cytokines upon 5-OP-RU stimulation while only ~10% of circulating MAIT cells were able to respond (Fig. 4b–d). After the macaques were treated, BAL MAIT cells in animals receiving 5-OP-RU rapidly lost the ability to respond to in vitro restimulation with 5-OP-RU, while MAIT cells in PBS treated macaques maintained their ability to produce cytokines (Fig. 4b–d). In contrast, PMA/ionomycin induced similar levels of cytokine production by MAIT cells in both PBS and 5-OP-RU treated macaques, although there was a trend for a reduction at very late time points in the 5-OP-RU treated animals (Fig. 4b–d). MAIT cells from pulmonary LNs, instillation site lesions in the lungs, the BAL and individually resected granulomas isolated at necropsy also showed a reduction in cytokine producing function after in vitro restimulation with 5-OP-RU and to a lesser extent after restimulation with PMA/ionomycin (Fig. 4e, f).

These data demonstrate several important points. First, prior to infection MAIT cell function after 5-OP-RU stimulation varies substantially between different tissues, with lung MAIT cells displaying higher levels of responsiveness compared to the cells in circulation. Second, treatment of Mtb infected macaques with 5-OP-RU leads to a striking reduction in pulmonary MAIT cell functionality. Last, the functional defect can be overcome to a certain extent if the TCR is bypassed via stimulation with second messengers like PMA/ionomycin. Therefore, rather than the expected increase in MAIT cell responses after 5-OP-RU treatment, MAIT cells entered an exhaustion-like state.

5-OP-RU treatment of Mtb infected macaques does not enhance conventional adaptive immune responses

We next examined the impact of 5-OP-RU treatment on the conventional adaptive immune response. We found that there was no difference in the kinetics of Mtb-specific CD4 T cell responses in the airways as measured by intracellular cytokine staining for IFN-γ and TNF-α after restimulation with Mtb peptide megapools (Fig. 5a, b). Likewise, there was no apparent impact of 5-OP-RU treatment on the kinetics of Mtb-specific CD8 T cells in the BAL (Fig. 5c, d). There was also no impact of 5-OP-RU administration on the magnitude of Mtb-specific CD4 and CD8 T cells in the blood, spleen, LNs, granulomas or instillation site lesions at necropsy (Fig. 5e, f). A previous study found that MAIT cells may directly provide help to B cells in rhesus macaques,[24] so we also measured Mtb-specific IgG responses in serum. However, there was no clear difference in antibody responses between treated and untreated animals (Fig. 5g). Collectively, these data show that stimulation of MAIT cells during Mtb infection did not boost Mtb-specific conventional adaptive immune responses.

Pulmonary 5-OP-RU treatment does not cause major alterations in the intestinal microbiota

Due to the role of MAIT cells at mucosal sites and the ability of MAIT cells to recognize microbe-derived molecules, a close interplay between MAIT cells and the microbiota has been hypothesized.[25] Indeed, recent work has demonstrated that the microbiota plays a critical role in the development of MAIT cells in mouse models.[6,26] Therefore, we sought to investigate if treatment with 5-OP-RU affects the microbiome. Fecal samples were collected from all 10 macaques prior to and following infection and treatment. The composition of the microbiota was characterized via 16 S rRNA sequencing. We found that alpha-diversity (with-in sample diversity) of the microbiota varied over the course of the experiment in both PBS and 5-OP-RU treated groups (Supplementary Fig. 1A, left panel). We did not find the alpha-diversities of the microbiome from the timepoints after PBS or 5-OP-RU treatement to be significantly different from each other or from their respective pre-infection and infected microbiomes (Supplementary Fig. 1A, right panel). Similarly, the community structure of the microbiota following 5-OP-RU treatment was not significantly different from that of PBS treated animals (Supplementary Fig. 1B). However, visualization of the relative abundance of microbial taxa over the experimental time course indicated alterations in the composition of the gut flora, albeit not consistent between animals within a treatment group (Supplementary Fig. 1C). Several taxa were identified to be differently abundant with comparing the PBS or 5-OP-RU treated animals to their respective pre-infection microbiomes (Supplementary Fig. 1D). Importantly, we found only three bacterial families, Gastranaerophilales, Family XIII and Paludibacteraceae to be enriched and one family, vadin BE97, to be depleted following 5-OP-RU treatment in comparison to PBS administration (Supplementary Fig. 1D). Overall, these analyses reveal that the 5-OP-RU treatment results in only minimal alterations in the intestinal microbiota of rhesus macaques.

PD-1 blockade partially restores MAIT cell function but not expansion after 5-OP-RU+CpG vaccination in uninfected macaques

We next examined whether macaque MAIT cells are able to expand after in vitro stimulation with 5-OP-RU. Peripheral blood mononuclear cells (PBMCs) isolated from uninfected animals were stimulated in vitro with 5-OP-RU for 6 days. Consistent with previous findings in pigtail macaques,[27] rhesus macaque MAIT cells proliferated similar to that of human MAIT cells during in vitro stimulation (Supplementary Fig. 2), indicating that macaque MAIT cells are not uniquely non-proliferative in response to TCR stimulation.

We next vaccinated uninfected macaques with 5-OP-RU+CpG using a lower dose of 5-OP-RU roughly equivalent to what we previously used in our murine model experiments (0.5 μg/kg) (Fig. 6a). This allowed us to test three possible explanations for the poor MAIT responses after 5-OP-RU treatment of Mtb infected macaques. First, treating uninfected macaques allowed us to ask if the Mtb infection itself inhibited the ability of MAIT cells to respond. Second, lowering the dose ten-fold allowed us to test the possibility that the results above were due to a high zone tolerance-like effect. Last, MAIT cells have been shown to be regulated by PD-1 during human TB,[28] so we included a group of macaques that received anti-PD-1 blocking antibody at the time of 5-OP-RU vaccination to ask if the upregulation of PD-1 was responsible for the poor MAIT cell responses in vivo.

5-OP-RU+CpG vaccination resulted in a striking upregulation of PD-1 in isotype control treated animals indicating that MAIT cells were effectively stimulated by this vaccination (Fig. 6b, c). PD-1 staining was greatly reduced on MAIT cells from animals treated with anti-PD-1, presumably as a consequence of cell surface PD-1 being occupied by the PD-1 blocking antibody (Fig. 6b, c). Similar to what was observed after treatment of Mtb infected macaques, MAIT cells failed to expand in the airways after vaccination, and anti-PD-1 treatment had no effect on MAIT cell frequencies (Fig. 6d). Although MAIT cells did not expand, Ki-67 was significantly upregulated on MAIT cells in both the BAL and blood after vaccination (Fig. 6e–h). PD-1 blockade along with vaccination may have slightly reduced Ki-67 expression in the BAL MAIT cells and delayed its peak expression in the circulating MAIT cells, but there was relatively little difference in Ki-67 expression in the

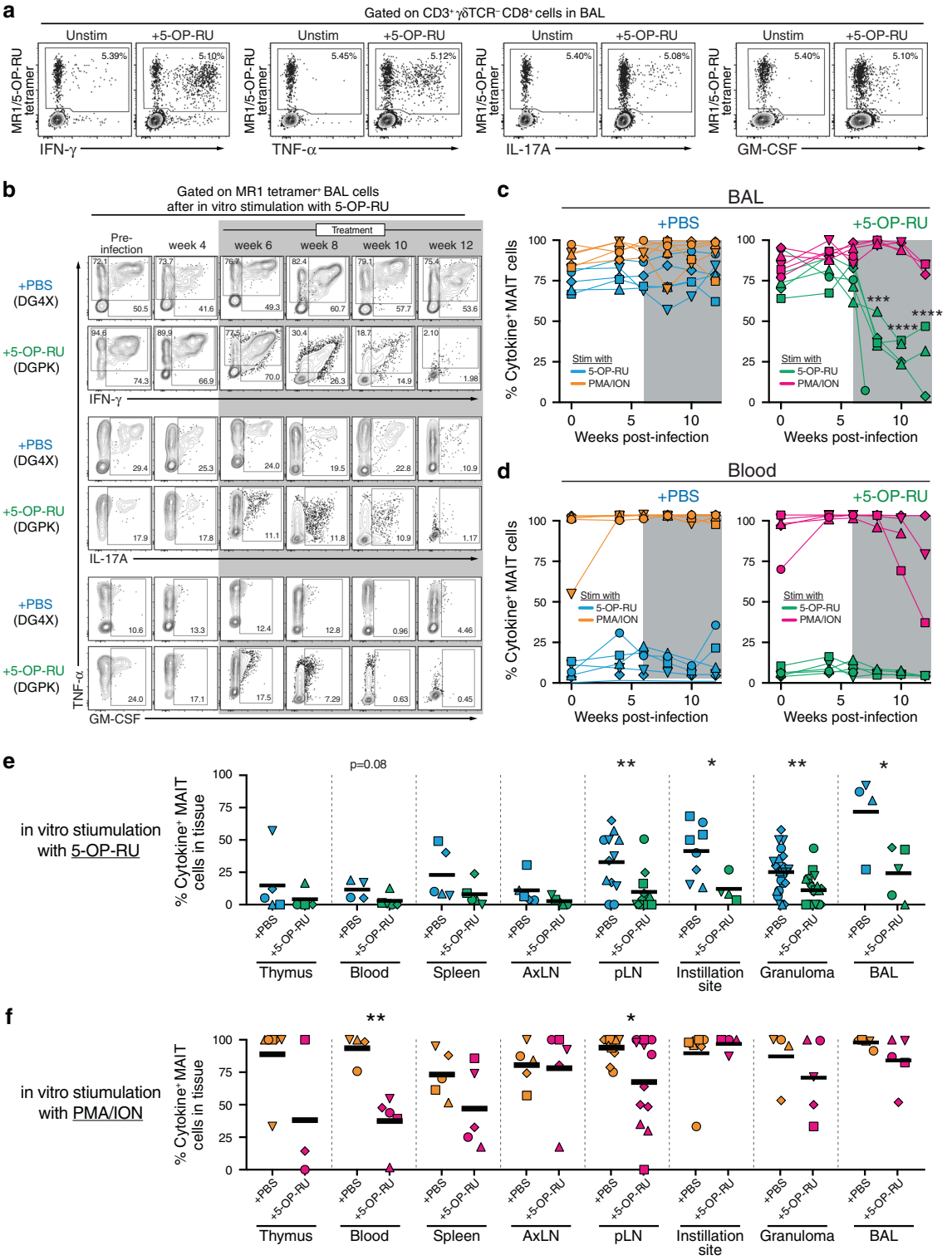

Fig. 4 5-OP-RU treatment leads to MAIT cell dysfunction in Mtb infected macaques. a Example FACS plots of intracellular cytokine staining of MR1/5-OP-RU tetramer$^+$ cells from the BAL (animal ID: DH4X) following in vitro stimulation with 5-OP-RU for 6 h. **b** Example FACS plots of intracellular cytokine staining of MAIT cells from the BAL following in vitro stimulation with 5-OP-RU. **c**, **d** Summary graphs of percentage of MAIT cells that are ether IFN-γ^+, TNF-α^+, IL-17A$^+$ or GM-CSF$^+$ in the BAL (**b**) or blood (**c**) following in vitro stimulation with 5-OP-RU or PMA/ionomycin (PMA/ION). **e**, **f** Graphs showing the percentage of MAIT cells that are ether IFN-γ^+, TNF-α^+, IL-17A$^+$, or GM-CSF$^+$ following in vitro stimulation with 5-OP-RU (**d**) or PMA/ionomycin (**e**) in the indicated tissues at necropsy. Each symbol represents an individual tissue sample from indicated animal. *$p < 0.05$, **$p < 0.01$, ***$p < 0.001$, ****$p < 0.0001$.

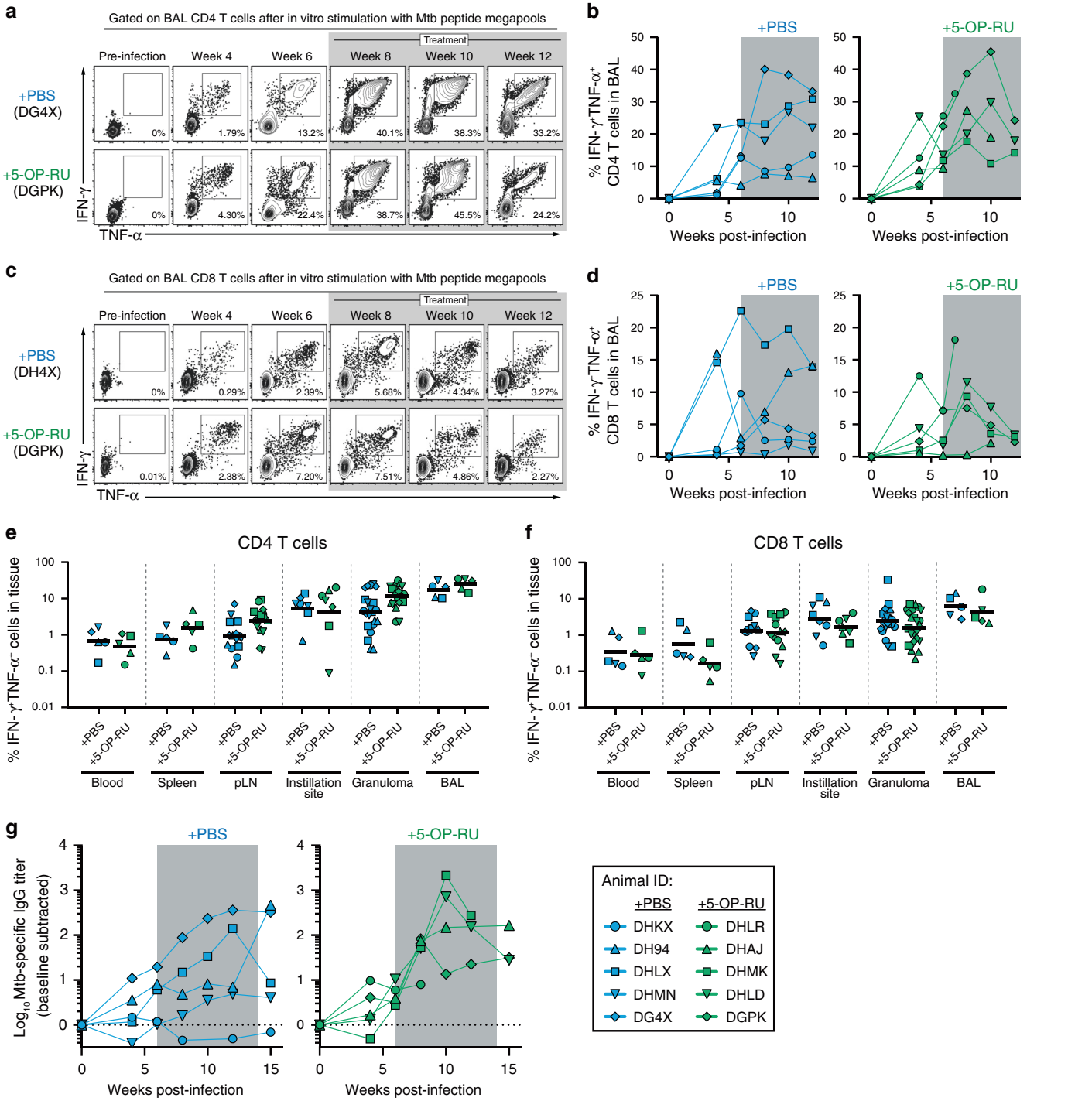

Fig. 5 5-OP-RU treatment of Mtb infected macaques does not enhance conventional adaptive immune responses. a Example FACS plots of intracellular cytokine staining of CD4 T cells from the BAL following in vitro stimulation with MTB300 peptide megapool. **b** Summary graphs of percentage of CD4 T cells in the BAL that are IFN-γ^+TNF-α^+ following in vitro stimulation. **c** Example FACS plots of intracellular cytokine staining of CD8 T cells from the BAL following in vitro stimulation with the MHC-I Mtb peptide megapool. **d** Summary graphs of percentage of CD8 T cells in the BAL that are IFN-γ^+TNF-α^+ following in vitro stimulation. Graphs showing the percentage of IFN-γ^+TNF-α^+ CD4 T cells (**e**) or CD8 T cells (**f**) in the indicated tissues at necropsy. Each symbol represents an individual tissue sample from indicated animal. **g** Mtb-specific antibody response following infection. Plasma levels of IgG specific to Mtb antigens were calculated by subtracting background values obtained in the pre-infection samples.

animals receiving anti-PD-1. Collectively, these data show that 5-OP-RU+CpG vaccination of rhesus macaques leads to MAIT cell recognition of the antigen and induces them to enter cell cycle but fails to result in their expansion.

At different time points after vaccination, we also restimulated cells from the airways with 5-OP-RU in vitro and measured MAIT cell functionality with intracellular cytokine staining. Again, we found that MAIT cells underwent a significant

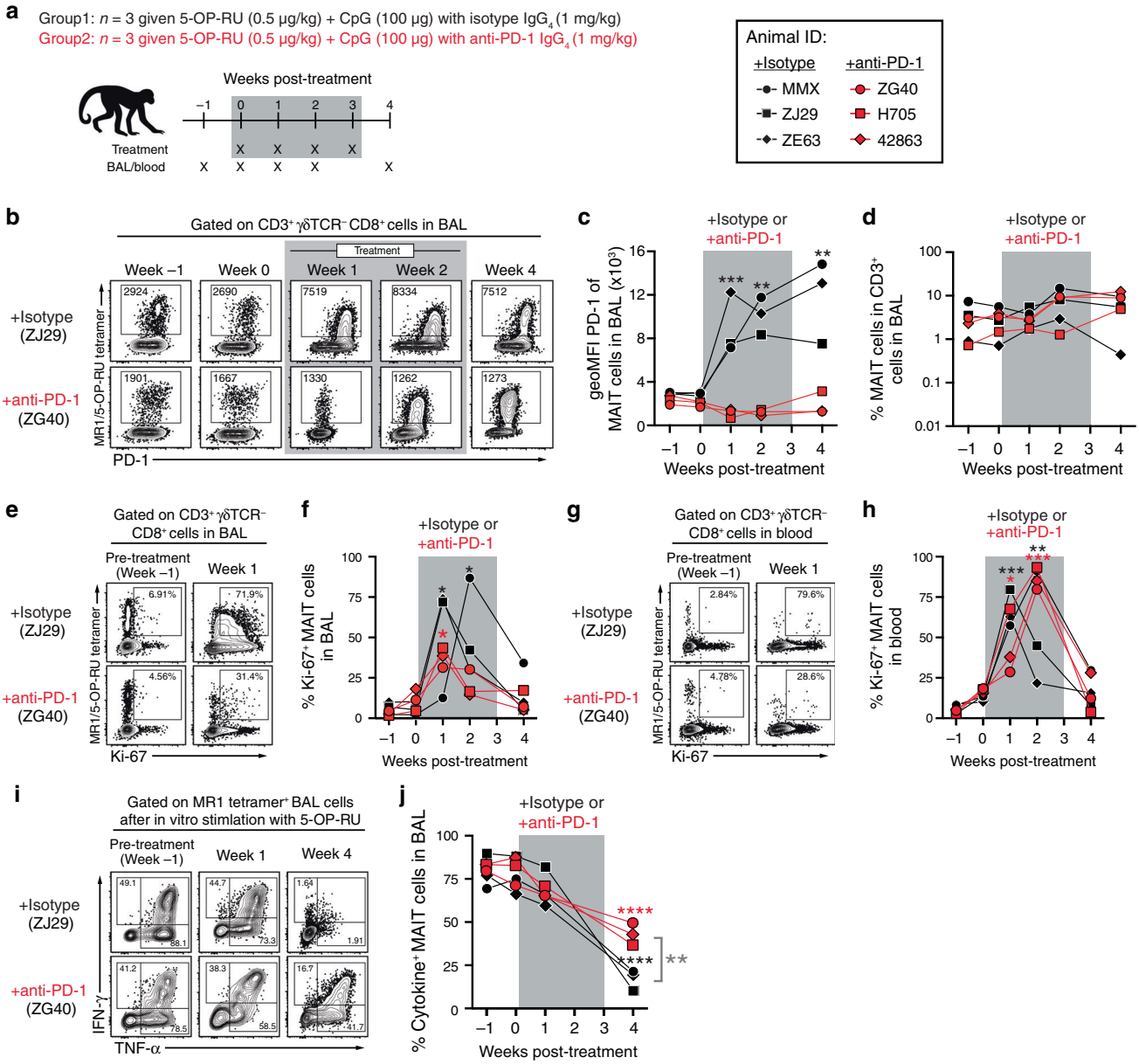

Fig. 6 PD-1 blockade partially restores MAIT cell function but not expansion after 5-OP-RU+CpG vaccination in uninfected macaques. **a** Uninfected animals were treated intratracheally with 5-OP-RU+CpG along with either rhesus macaque IgG_4 isotype control or primatized anti-PD-1 antibody. **b** Example FACS plots of PD-1 expression on MAIT cells in the BAL. **c** Summary graph showing the geoMFI of PD-1 on MAIT cells in the BAL. **d** Kinetics of the frequency of MAIT cells among $CD3^+$ cells in the BAL. **e** Example FACS plots of Ki-67 expression on MAIT cells in the BAL from pre-treatment and week 1 post-treatment. **f** Percentage of Ki-67^+ MAIT cells in the BAL. **g** Example FACS plots of Ki-67 expression on MAIT cells in the blood from pre-treatment and week 1 post-treatment. **h** Percentage of Ki-67^+ MAIT cells in the blood. **i** Example FACS plots of intracellular cytokine staining of MAIT cells from the BAL following in vitro stimulation with 5-OP-RU. **J** Percentage of MAIT cells that are ether IFN-γ^+, TNF-α^+ or IL-$17A^+$ in the BAL following in vitro stimulation with 5-OP-RU. *$p < 0.05$, **$p < 0.01$, ***$p < 0.001$, ****$p < 0.0001$.

reduction in their cytokine producing potential after 5-OP-RU administration (Fig. 6i, j). Interestingly, PD-1 blockade partially rescued the function of MAIT cells at 4 weeks post-treatment, indicating that loss of effector functions but not proliferation was in part due to PD-1 expression. Thus, the lack of MAIT cell expansion and antigen-driven reduction in MAIT cell functionality was not due to the presence of the Mtb infection and was very similar despite a 10-fold reduction in 5-OP-RU dose. Moreover, PD-1 expression was partly responsible for the loss of MAIT cell function but had no role in their poor expansion.

DISCUSSION

We previously showed that treating Mtb infected mice with the MAIT cell TCR agonist 5-OP-RU leads to a large expansion of MAIT cells and reduction in lung bacterial loads,[14] prompting us to further evaluate the translatability of MAIT cell directed therapy during TB in the rhesus macaque model. While no control animals were lost prior to the predetermined endpoint, three of five treated animals developed distress relating to bronchoconstriction after 5-OP-RU instillation and needed to be humanly euthanized early. In all cases this appeared to be due to enlarged LNs impinging on airways, so 5-OP-RU treatment may have

exacerbated disease in these animals. However, rhesus macaques have been shown to be particularly prone to developing TB lymphadenopathy,[21,22] and bacterial loads were not substantially increased in the animals that developed early disease. Although small effects can be difficult to detect with the groups sizes that can be achieved in aBSL3 NHP studies, there was no obvious biological effect on MAIT cells to which we could ascribed the lymph node disease in the treated animals. Therefore, we interpret this result with caution. A larger study would be needed to more definitively establish a causal link between 5-OP-RU treatment and lymphadenopathy in macaques. Regardless, it is clear 5-OP-RU treatment in macaques did not lead to the beneficial outcomes we observed in mice. 5-OP-RU treatment failed to expand MAIT cells and instead only drove them into a functionally exhausted-like state. This was not a result of the Mtb infection, as vaccination of uninfected macaques by instillation of 5-OP-RU (adjuvanted with CpG) into the lungs also did not increase the frequency of MAIT cells and likewise resulted in their loss of cytokine producing ability. Functional inactivation of MAIT cells following in vivo administration of 5-OP-RU during TB and vaccination was associated with upregulation of the co-inhibitory receptor PD-1. Therefore, we asked if PD-1 blockade could boost MAIT cell responses following pulmonary 5-OP-RU+CpG vaccination. While PD-1 blockade did not result in MAIT cell expansion, it did partly alleviate their loss of function. Therefore, rather than the expansion of MAIT cells normally seen in mice after administration of 5-OP-RU, in rhesus macaques MAIT cells fail to proliferate and undergo functional inactivation of their cytokine producing activity. Our study reveals an important conundrum. That is, while MAIT cells are very weakly stimulated by Mtb infection,[14,15,23,29] attempting to drive MAIT responses by treating macaques with additional TCR ligand only decreases their functionality.

Previous studies have documented defects in MAIT cell function during infection, cancer and sepsis.[30–39] Our data showing MAIT cell functional defects directly resulting from TCR stimulation indicates that part of the MAIT dysfunction observed in these settings may result from increased MAIT antigen stimulation, rather than disease-related bystander processes. The loss of MAIT cell function that occurs in these reports and here after 5-OP-RU treatment resembles the exhaustion of virus and tumor-specific conventional CD8 T cells. However, it is unclear if this is the same phenomena for several reasons. Exhaustion of conventional CD8 T cells is a unique differentiation state that occurs during a period of chronic antigenic stimulation following an initial clonal burst of highly functional effector cells.[40] Following 5-OP-RU treatment, MAIT cells never underwent an expansion phase. They simply began to lose effector functions quickly after in vivo stimulation. Moreover, the ability of MAIT cells in different tissues to produce cytokine following 5-OP-RU stimulation is highly variable, confounding comparisons to exhaustion. At baseline, MAIT cells in the BAL were the most functional and those in the blood the least. Even after lung MAIT cells had undergone this functional inactivation, they still produced more cytokine than blood cells prior to treatment. In other words, it is difficult to call lung MAIT cells exhausted if their counterparts in circulation are even less functional at their best. Therefore, it is not clear if the pulmonary MAIT cells present after 5-OP-RU treatment are truly exhausted as understood for conventional T cells. In future experiments, it will be important to molecularly characterize MAIT cells before and after 5-OP-RU-treatment in vivo to identify mechanisms leading to their dysfunction and better understand the nature of this unusual T cell inactivation process.

PD-1 is a key mediator of the exhaustion of conventional peptide-specific CD8 T cells, and several biologics targeting PD-1 or its ligands are used in the treatment of various cancers. Here we saw a striking upregulation of PD-1 on MAIT cells in the lungs as well as circulation after 5-OP-RU treatment. PD-1 blockade during 5-OP-RU+CpG vaccination did at least partly prevent the reduction in MAIT cell function. Therefore, while PD-1 does have a role in MAIT dysfunction, it seems likely that other regulatory pathways also have significant contributions to the downregulation of MAIT cell effector functions after in vivo stimulation. Interestingly, the defect in cytokine production after 5-OP-RU treatment of Mtb infected animals was only observed when the cells were restimulated with 5-OP-RU, and the cells displayed equivalent cytokine production as controls upon PMA/ionomycin restimulation, indicating that the defect relates to signaling through the TCR. It is possible that multiple co-inhibitory receptors cooperate in MAIT cell inactivation, as MAIT cells have been shown to express several different immune checkpoint molecules.[32,34,35,41,42]

Our original goal was to drive large populations of MAIT cells in the lungs of macaques and examine the impact on Mtb infection. However, MAIT cells failed to increase in number after instillation of 5-OP-RU, and PD-1 blockade during antigenic stimulation did not lead to MAIT cell expansion. In mice, MAIT cells can readily be driven to expand ~100 fold, as long as 5-OP-RU is properly adjuvanted.[7,12,14–16] Unlike mice, it is not clear that NHP or human MAIT cells are able to undergo similar dramatic expansions in vivo. Studies of human vaccination with *Shigella dysenteriae* 1[43] or BCG,[18] as well as controlled human bacterial infection studies with *Salmonella enterica* serovar Typhi[44] and *S. enterica* serovar Paratyphi A[45] have consistently found that MAIT cells become activated but do not expand in number after bacterial infection. MAIT cells in the circulation are also reduced rather than expanded in patients with TB, sepsis and COVID-19.[10,33,36–39,46,47] MAIT cells may accumulate to slightly higher frequencies in tissues during some infections as has been shown in the BAL during TB or peritoneal cavity during spontaneous bacterial peritonitis,[48,49] but given the small magnitude of changes reported this could be explained by recruitment from circulation rather than TCR-driven expansion. Based on the results presented here, it seems likely that MAIT cells do not mount large proliferative responses in humans and NHPs as part of their typical response to antigenic stimulation. In other words, our data raise the hypothesis that the lack of proliferation and downregulation of cytokine producing ability after strong antigenic challenge may not represent a defect but normal MAIT cell biology in vivo in humans and NHPs. That is not to diminish the importance of MAIT cells in host defense, as human MAIT cell deficiency has been shown to lead to increased susceptibility to viral and bacterial infections.[50] We suggest the lack of MAIT cell responses reported here and in the above-mentioned literature is a beneficial adaptation of MAIT cells specifically in response to sudden and large increases in TCR ligand availability. Given that MAIT cells are likely persistently stimulated by antigens derived from the microbiota, there may be multiple checkpoints put on their ability to expand in number through large clonal bursts and produce inflammatory cytokines in order to prevent immunopathology.

It is not clear why the outcome of 5-OP-RU treatment of Mtb infection is so different in mice versus macaques. This may reflect a fundamental difference in MAIT cell biology between the two species or even differences in their precursor frequency. However, it could also be due to differences in MAIT cell extrinsic factors such as the microbiota composition or MAIT cell stimulation history. For example, at baseline murine MAIT cells in SPF mice are very low or negative for PD-1, while MAIT cells in macaques express significant levels of PD-1, indicating that there may be major differences in the levels of ambient TCR signaling between mice and NHPs. Therefore, mouse and macaque MAIT cells in the lungs may be in different functional states due to differences in the levels of persistent TCR stimulation at homeostasis. Additional studies are needed to better understand the mechanisms that regulate MAIT cell expansion in macaques so that strategies to induce large populations of MAIT cells in vivo can be developed, assuming a large number of activated MAIT cells is safe in NHPs

and humans. We found that 5-OP-RU instillation led to a striking upregulation of Ki-67 in MAIT cells in both lung and blood, indicating that MAIT cells were likely induced to enter cell cycle. A reasonable hypothesis is that MAIT cell turnover was balanced by cell death, resulting in no net increase in cell number. It is possible that other adjuvants or different antigen delivery dynamics (e.g., sustained low level 5-OP-RU stimulation) may lead to MAIT cell expansion in vivo. Last, we have only used one MAIT antigen in this study, so it will be important to test other MR1 ligands for their ability to drive MAIT cell expansion in macaques.

Given the inability to expand MAIT cells, we could not test the hypothesis that large populations of MAIT cells can be protective against TB in this macaque study. Therefore, it remains possible that MAIT cell targeting therapies can be beneficial in Mtb infection, but this study highlights the significant barriers to exploring the role of MAIT cell-based therapeutics and vaccinations in vivo. Although the mouse model is a powerful tool that has revealed much about MAIT cell biology,[51] there may be important instances where MAIT cell responses in mice may not be representative of responses in macaques and by extension also not representative of in vivo MAIT cell responses in humans. These data indicate it is important that hypotheses regarding MAIT cell biology that are developed in mice be further explored in humans if possible and NHP models when needed. The development of strategies to induce large populations of highly functional MAIT cells in macaques is needed to evaluate their clinical potential as targets of vaccines and therapeutics in humans.

MATERIALS AND METHODS

Rhesus macaques

Sixteen healthy rhesus macaques originally from the NIAID breeding colony on Morgan Island were selected for this study and were tuberculin skin test negative. Animals were housed in nonhuman primate biocontainment racks and maintained in accordance with the Animal Welfare Act, the Guide for the Care and Use of Laboratory Animals and all applicable regulations, standards, and policies in a fully AAALAC International accredited Animal Biosafety Level 3 vivarium. All procedures were performed utilizing appropriate anesthetics as listed in the NIAID DIR Animal Care and Use Committee (ACUC) approved animal study proposal LPD-25E. Euthanasia methods were consistent with the AVMA Guidelines on Euthanasia and endpoint criteria listed in the NIAID DIR ACUC approved animal study proposal LPD-25E.

Human blood donors

Blood samples of healthy volunteers were obtained from the NIH Blood Bank under Institutional Review Board-approved protocols of both the NIAID and the Department of Transfusion Medicine. PBMCs were isolated by Ficoll-Paque (GE Life Sciences) density centrifugation and stored at −80 °C until later use.

Mtb infection and 5-OP-RU treatment

Animals were infected with 120–150 colony forming units (CFU) of a H37*Rv* strain of Mtb. For infection, animals were anesthetized and 2 ml of PBS containing the bacteria were bronchoscopically-instilled into the right lower lung lobe. Infection dose was confirmed by plating of aliquots onto 7H11 agar plates. For the treatment during Mtb infection, 5 µg/kg of body weight of 5-OP-RU[14] diluted in 2 ml of PBS was administrated intratracheally once per week for 9 weeks beginning at 6 weeks post-infection. In PD-1 blockade experiment, uninfected animals were treated intratracheally once per week for 4 weeks with 0.5 µg/kg of body weight of 5-OP-RU and 100 µg of CpG ODN 2006 (InvivoGen) mixed with 10 mg/kg of body weight of either rhesus macaque IgG_4 isotype control antibody (DSPR4) obtained from the NHP Reagent Resource or anti-PD-1 antibody (humanized clone EH12 kappa variable domains with rhesus macaque kappa and IgG_4 constant regions).[52]

PET/CT scanning and data analysis

Rhesus were imaged prior to infection and every two weeks beginning at 5 weeks post-infection for a maximum of 7 PET/CT scans (Fig. 1a). The imaging studies were conducted with an optimized [^{18}F]-FDG dose (0.5 mCi/kg) administered intravenously as previously described.[53] A 360-projection CT scan of the lungs was acquired during a ~50 s breath hold on a LFER 150 PT/CT scanner (Mediso Inc, Budapest, Hungary). A 20-minute PET dataset/per field of view was acquired during mechanical ventilation and the raw CT and PET data were reconstructed using the Nucline software (Mediso, Inc, Budapest, Hungary) to create individual DICOM files that were co-registered using MIM Maestro (v. 6.2, MIM Software Inc, Cleveland, Ohio). A lung volume of interest (VOI) was defined on the CT image and the VOI was transferred to the PET image as previously described to determine the total [^{18}F]-FDG uptake referred to as the lung total lesion glycolysis (TLG).[53] The analysis of disease burden included abnormal TLG of the lung, and a consistent region of the hylar and subcarinal LNs of each animal with standardized uptake value above background. The pulmonary LN [^{18}F]-FDG uptake was measured by creating a VOI in MIM in the LN with uptake in the region surrounding the carina as described by White et al.[54]. Two readers independently performed image analysis for each animal. Three-dimensional projections were generated using Osirix v 5.9 software (Pixmeo, Geneva, Switzerland).

Two approaches were taken for measuring the bronchial constriction observed in the infected animals. In the first, the diameters of the most constricted region of main right and left bronchi lumens were measured on the axial plane of CT scan with the embedded MIM ruler tool from anterior to posterior and from left to right. The measurements were compared to the baseline scan measurements at that axial plane to calculate a percentage of occlusion. The resulting percentages were averaged to get the mean percentage of occlusion at each time point. In the second method, the volume of the bronchus from the carinal bifurcation to 2.3 cm below from the carinal bifurcation (the area observed to contain the regions of occlusion in the macaques on study) was calculated by using the region grow feature of MIM set to capture the bronchi lumen (HU -1024 to -700) which was manually adjusted if small airway regions were missed by the program. The volumes of the right and left lumens were added together and compared to the baseline combined volume of the bronchi, and the percentage occlusion calculated. See also Supplementary Fig. 3.

Cell isolation and in vitro stimulation

Blood samples were collected in EDTA tubes and PBMCs were isolated by Ficoll-Paque density centrifugation. BAL samples were passed through a 100 µm cell strainer, pelleted, and counted for analysis. Lung lobes and tracheal/bronchial tissues were minced using a GentleMACS Tissue Dissociator (Miltenyi Biotec) and were enzymatically digested in a shaker incubator at 37 °C for 40 min in RPMI medium containing 1 mg/ml Collagenase D (Roche-Diagnostics), 1 mg/ml hyaluronidase and 50 U/ml DNase I (Sigma Aldrich). Suspensions were then passed through a 100 µm cell strainer and enriched for lymphocytes using a 40% Percoll density gradient centrifugation. Lymph nodes and spleens were dissociated using a GentleMACS Tissue Dissociator. Granulomas were individually resected from the lungs and samples used for flow cytometry analysis were pushed through a 100 µm cell strainer. Aliquots from all samples were serially diluted and plated on 7H11 agar plates for CFU quantification. Cells were stimulated in X-vivo 15 media (Lonza) supplemented with 10% FCS at 37 °C with either PMA/ionomycin (Leukocyte activation cocktail, BD Biosciences) for 3 hours, 5OP-RU (50 nM) or MHC-I[37] and MHC-II (MTB300)[55] Mtb peptide megapools (1 µg/ml and 2 µg/ml respectively) for 6 hours in the presence of brefeldin A and monensin (eBioscience). To assess in vitro cell proliferation, cryopreserved PBMCs from the uninfected animals (ID: MMX, ZJ29, ZE63, ZG40, H705, 42863) before 5-OP-RU treatment or human healthy donors were thawed and cultured at 5×10^6 cells/ml in X-vivo 15 media supplemented with 10% FCS,10 ng/ml recombinant human IL-2, 100 U/ml penicillin, 100 µg/ml streptomycin, and 2 µg/ml amphotericin B. Cells were stimulated with 10 nM 5-OP-RU and the fresh media (without 5-OP-RU) were added every 2 days. On day 6, cells were harvested for analysis as described below.

Flow cytometry

Tetramer stains were performed by incubating 1×10^6 cells at 37 °C for 30 min with rhesus macaque MR1/5-OP-RU tetramer in X-vivo 15 media containing 10% FCS and monensin. Tetramers were produced by the NIAID tetramer core facility (Emory University, GA). Fluorochrome-labeled antibodies used for flow cytometric analysis are listed in Supplementary Table 1. Surface antigens and dead cells were stained in PBS + 1% FCS + 0.1% sodium azide for 20 min at 4 °C. For intracellular cytokine and

transcription factor staining, cells were fixed and permeabilized with the Foxp3 Transcription Factor Staining Buffer Kit (eBioscience) and stained for 1 h at 4 °C. Samples were acquired on a FACSymphony (BD Biosciences), and data were analyzed using FlowJo 10 (Treestar).

Measurement of Mtb-specific IgG titer

Ninety-six-well ELISA plates were coated with Mtb whole cell lysate (strain H37Rv, BEI Resources) at 10 µg/ml diluted in PBS for 1 h at 37 °C. The plates were washed and blocked overnight at 4 °C with block buffer (5% milk powder + 4% whey buffer in PBS Tween-20). Plates were then washed, and plasma samples were added at a serial 1:3 dilutions starting at a 1:10 dilution with 4% whey buffer and incubated for 1 h at 37 °C. After washing, plates were incubated with goat anti-monkey IgG (H + L)-HRP (Novus Bio) was added at 1:1000 dilution in 4% whey buffer for 1 h at 37 °C. Plates were washed and 1-Step Ultra-TMB ELISA Substrate Solution (Thermo Scientific) was added to develop the plates. The reaction was stopped by adding 0.5 M sulfuric acid, and the OD measured at 450 nm. The OD value of each pre-infection baseline was subtracted from each post-infection timepoint sample in order to calculate Mtb-specific IgG levels.

Microbiota analyses

One pre-infection fecal sample was collected 2 to 4 weeks prior to infection and another on the day of infection. Additional samples were collected at weeks 4, 8, 12 post-infection and at necropsy. All samples were stored at −80 °C until completion of experiment. DNA was extracted from ~0.05 g of fecal material using QIAamp Fast DNA stool Mini kit (Qiagen, Hilden, Germany) and the V4 region of the 16 s rRNA gene was amplified with primers 5′-TCGTCGGCAGCGTCAGATGTGTATAAGAGACAGGTGCCAGC MGCCGCGGTAA-3′ and 5′-GTCTCGTGGGCTCGGAGATGTGTATAAGAGACAG GGACTACHVGGGTWTCTAAT-3′ and sequenced as previously described.[56] The raw reads were demultiplexed, denoised and filtered for chimeras using the DADA2/QIIME2 pipeline (version 2-2020.2).[57] The processed data resulted in an average of ~55,000 reads/sample. Alpha and beta-diversity analyses were performed using Shannon and Bray-Curtis dissimilarity indices respectively on read data rarefied to a depth of 40,000 reads/sample. Taxonomic classification was performed utilizing QIIME2 and the Silva database release 132.[58] Differentially abundant taxa were identified using Linear discriminant analysis (LefSe) and filtered for linear discriminant score (LDA) > 2 and p value < 0.05[59].

Quantification and statistical analysis

All analyses were conducted using Prism 8 (GraphPad Software). Two-sample t test was used for two group comparisons and ANOVA was used for comparing multiple groups. Unless specifically denoted in the Figures, a p value < 0.05 was considered statistically significant. Data are presented as mean ± SEM.

REFERENCES

1. Godfrey, D. I., Koay, H. F., McCluskey, J. & Gherardin, N. A. The biology and functional importance of MAIT cells. *Nat. Immunol.* **20**, 1110–1128 (2019).
2. Keller, A. N., Corbett, A. J., Wubben, J. M., McCluskey, J. & Rossjohn, J. MAIT cells and MR1-antigen recognition. *Curr. Opin. Immunol.* **46**, 66–74 (2017).
3. Corbett, A. J. et al. T-cell activation by transitory neo-antigens derived from distinct microbial pathways. *Nature* **509**, 361–365 (2014).
4. Treiner, E. et al. Selection of evolutionarily conserved mucosal-associated invariant T cells by MR1. *Nature* **422**, 164–169 (2003).
5. Lantz, O. & Legoux, F. MAIT cells: an historical and evolutionary perspective. *Immunol. Cell Biol.* **96**, 564–572 (2018).
6. Constantinides, M. G. et al. MAIT cells are imprinted by the microbiota in early life and promote tissue repair. *Science* **366**, eaax6624 (2019).
7. Hinks, T. S. C. et al. Activation and In Vivo Evolution of the MAIT Cell Transcriptome in Mice and Humans Reveals Tissue Repair Functionality. *Cell Rep.* **28**, 3249–3262 e3245 (2019).
8. Leng, T. et al. TCR and inflammatory signals tune human MAIT cells to exert specific tissue repair and effector functions. *Cell Rep.* **28**, 3077–3091 e3075 (2019).
9. Meierovics, A., Yankelevich, W. J. & Cowley, S. C. MAIT cells are critical for optimal mucosal immune responses during in vivo pulmonary bacterial infection. *Proc. Natl Acad. Sci. USA* **110**, E3119–3128 (2013).
10. Le Bourhis, L. et al. Antimicrobial activity of mucosal-associated invariant T cells. *Nat. Immunol.* **11**, 701–708 (2010).
11. Wang, H. et al. MAIT cells protect against pulmonary Legionella longbeachae infection. *Nat. Commun.* **9**, 3350 (2018).
12. Chen, Z. et al. Mucosal-associated invariant T-cell activation and accumulation after in vivo infection depends on microbial riboflavin synthesis and co-stimulatory signals. *Mucosal Immunol.* **10**, 58–68 (2017).
13. Joosten, S. A. et al. Harnessing donor unrestricted T-cells for new vaccines against tuberculosis. *Vaccine* **37**, 3022–3030 (2019).
14. Sakai, S. et al. MAIT cell-directed therapy of *Mycobacterium tuberculosis* infection. *Mucosal Immunol.* **14**, 199–208 (2021).
15. Yu, H. et al. Artificially induced MAIT cells inhibit *M. bovis* BCG but not *M. tuberculosis* during in vivo pulmonary infection. *Sci. Rep.* **10**, 13579 (2020).
16. Vorkas, C. K. et al. Efficient 5-OP-RU-induced enrichment of Mucosal-associated invariant T cells in the murine lung does not enhance control of aerosol *Mycobacterium tuberculosis* infection. *Infect. Immun.* **89**, e00524–20 (2020).
17. Rahimpour, A. et al. Identification of phenotypically and functionally heterogeneous mouse mucosal-associated invariant T cells using MR1 tetramers. *J. Exp. Med* **212**, 1095–1108 (2015).
18. Suliman, S. et al. MR1-Independent Activation of Human Mucosal-Associated Invariant T Cells by Mycobacteria. *J. Immunol.* **203**, 2917–2927 (2019).
19. Greene, J. M. et al. MR1-restricted mucosal-associated invariant T (MAIT) cells respond to mycobacterial vaccination and infection in nonhuman primates. *Mucosal Immunol.* **10**, 802–813 (2017).
20. Scanga, C. A. & Flynn, J. L. Modeling tuberculosis in nonhuman primates. *Cold Spring Harb. Perspect. Med* **4**, a018564 (2014).
21. Ganchua, S. K. C. et al. Lymph nodes are sites of prolonged bacterial persistence during *Mycobacterium tuberculosis* infection in macaques. *PLoS Pathog.* **14**, e1007337 (2018).
22. Maiello, P. et al. Rhesus macaques are more susceptible to progressive tuberculosis than cynomolgus macaques: a quantitative comparison. *Infect. Immun.* **86**, e00505–17 (2018).
23. Kauffman, K. D. et al. Limited pulmonary mucosal-associated invariant T cell accumulation and activation during *Mycobacterium tuberculosis* infection in rhesus macaques. *Infect. Immun.* **86**, e00431–18 (2018).
24. Rahman, M. A. et al. Mucosal-associated invariant T (MAIT) cells provide B-cell help in vaccinated and subsequently SIV-infected Rhesus Macaques. *Sci. Rep.* **10**, 10060 (2020).
25. Oh, J. & Unutmaz, D. Immune cells for microbiota surveillance. *Science* **366**, 419–420 (2019).
26. Legoux, F. et al. Microbial metabolites control the thymic development of mucosal-associated invariant T cells. *Science* **366**, 494–499 (2019).
27. Juno, J. A. et al. MAIT cells upregulate alpha4beta7 in response to acute simian immunodeficiency virus/simian HIV infection but are resistant to peripheral depletion in pigtail macaques. *J. Immunol.* **202**, 2105–2120 (2019).
28. Jiang, J. et al. Mucosal-associated invariant T-cell function is modulated by programmed death-1 signaling in patients with active tuberculosis. *Am. J. Respir. Crit. Care Med* **190**, 329–339 (2014).
29. Bucsan, A. N. et al. Mucosal-activated invariant T cells do not exhibit significant lung recruitment and proliferation profiles in macaques in response to infection with *Mycobacterium tuberculosis* CDC1551. *Tuberculosis (Edinb.)* **116S**, S11–S18 (2019).
30. Leeansyah, E. et al. Activation, exhaustion, and persistent decline of the antimicrobial MR1-restricted MAIT-cell population in chronic HIV-1 infection. *Blood* **121**, 1124–1135 (2013).
31. Hengst, J. et al. Nonreversible MAIT cell-dysfunction in chronic hepatitis C virus infection despite successful interferon-free therapy. *Eur. J. Immunol.* **46**, 2204–2210 (2016).
32. Duan, M. et al. Activated and exhausted MAIT cells foster disease progression and indicate poor outcome in hepatocellular carcinoma. *Clin. Cancer Res* **25**, 3304–3316 (2019).
33. Trivedi, S. et al. Mucosal-associated invariant T (MAIT) cells mediate protective host responses in sepsis. *Elife* **9**, e55615 (2020).
34. Huang, W. et al. Mucosal-associated invariant T-cells are severely reduced and exhausted in humans with chronic HBV infection. *J. Viral Hepat.* **27**, 1096–1107 (2020).
35. Ellis, A. L. et al. MAIT cells are functionally impaired in a Mauritian cynomolgus macaque model of SIV and Mtb co-infection. *PLoS Pathog.* **16**, e1008585 (2020).
36. Parrot, T. et al. MAIT cell activation and dynamics associated with COVID-19 disease severity. *Sci Immunol* **5**, eabe1670 (2020).
37. Pomaznoy, M. et al. Quantitative and qualitative perturbations of CD8(+) MAITs in healthy mycobacterium tuberculosis-infected individuals. *Immunohorizons* **4**, 292–307 (2020).
38. Wong, E. B. et al. Low levels of peripheral CD161++CD8+ mucosal associated invariant T (MAIT) cells are found in HIV and HIV/TB co-infection. *PLoS One* **8**, e83474 (2013).
39. Kwon, Y. S. et al. Mucosal-associated invariant T cells are numerically and functionally deficient in patients with mycobacterial infection and reflect disease activity. *Tuberculosis (Edinb.)* **95**, 267–274 (2015).

40. McLane, L. M., Abdel-Hakeem, M. S. & Wherry, E. J. CD8 T cell exhaustion during chronic viral infection and cancer. *Annu Rev. Immunol.* **37**, 457–495 (2019).
41. Dias, J., Leeansyah, E. & Sandberg, J. K. Multiple layers of heterogeneity and subset diversity in human MAIT cell responses to distinct microorganisms and to innate cytokines. *Proc. Natl Acad. Sci. USA* **114**, E5434–E5443 (2017).
42. Wang, H. et al. IL-23 costimulates antigen-specific MAIT cell activation and enables vaccination against bacterial infection. *Sci. Immunol.* **4**, eaaw0402 (2019).
43. Le Bourhis, L. et al. MAIT cells detect and efficiently lyse bacterially-infected epithelial cells. *PLoS Pathog.* **9**, e1003681 (2013).
44. Salerno-Goncalves, R. et al. Challenge of Humans with Wild-type *Salmonella enterica* Serovar Typhi Elicits Changes in the Activation and Homing Characteristics of Mucosal-Associated Invariant T Cells. *Front Immunol.* **8**, 398 (2017).
45. Howson, L. J. et al. MAIT cell clonal expansion and TCR repertoire shaping in human volunteers challenged with *Salmonella* Paratyphi A. *Nat. Commun.* **9**, 253 (2018).
46. Grimaldi, D. et al. Specific MAIT cell behaviour among innate-like T lymphocytes in critically ill patients with severe infections. *Intensive Care Med* **40**, 192–201 (2014).
47. Gold, M. C. et al. Human mucosal associated invariant T cells detect bacterially infected cells. *PLoS Biol.* **8**, e1000407 (2010).
48. Ibidapo-Obe, O. et al. Mucosal-Associated Invariant T Cells Redistribute to the Peritoneal Cavity During Spontaneous Bacterial Peritonitis and Contribute to Peritoneal Inflammation. *Cell Mol. Gastroenterol. Hepatol.* **9**, 661–677 (2020).
49. Wong, E. B. et al. TRAV1-2(+) CD8(+) T-cells including oligoconal expansions of MAIT cells are enriched in the airways in human tuberculosis. *Commun. Biol.* **2**, 203 (2019).
50. Howson, L. J. et al. Absence of mucosal-associated invariant T cells in a person with a homozygous point mutation in MR1. *Sci. Immunol.* **5**, eabc9492 (2020).
51. Wang, H., Chen, Z., McCluskey, J. & Corbett, A. J. Mouse models illuminate MAIT cell biology. *Mol. Immunol.* **130**, 55–63 (2020).
52. Mylvaganam, G. H. et al. Combination anti-PD-1 and antiretroviral therapy provides therapeutic benefit against SIV. *JCI Insight* **3**, e122940 (2018).
53. Kauffman, K. D. et al. Defective positioning in granulomas but not lung-homing limits CD4 T-cell interactions with *Mycobacterium tuberculosis*-infected macrophages in rhesus macaques. *Mucosal Immunol.* **11**, 462–473 (2018).
54. White, A. G. et al. Analysis of 18FDG PET/CT Imaging as a tool for studying mycobacterium tuberculosis infection and treatment in non-human primates. *J. Vis. Exp.* 56375 (2017).
55. Lindestam Arlehamn, C. S. et al. A quantitative analysis of complexity of human pathogen-specific CD4 T cell responses in healthy *M. tuberculosis* infected South Africans. *PLoS Pathog.* **12**, e1005760 (2016).
56. Namasivayam, S. et al. Longitudinal profiling reveals a persistent intestinal dysbiosis triggered by conventional anti-tuberculosis therapy. *Microbiome* **5**, 71 (2017).
57. Caporaso, J. G. et al. QIIME allows analysis of high-throughput community sequencing data. *Nat. Methods* **7**, 335–336 (2010).
58. Quast, C. et al. The SILVA ribosomal RNA gene database project: improved data processing and web-based tools. *Nucleic Acids Res.* **41**, D590–596 (2013).
59. Segata, N. et al. Metagenomic biomarker discovery and explanation. *Genome Biol.* **12**, R60 (2011).

ACKNOWLEDGEMENTS

We are grateful to Dr. Rashida Moore and Dr. Richard Herbert for providing veterinary care for animals in this study. We thank all staff members of the National Institutes of Allergy and Infectious Diseases (NIAID), Comparative Medicine Branch Animal Biosafety Level 3 facility for their technical support. This work was supported by the Intramural Research Program of the NIAID. G.J.F. is supported by P01AI056299 and R37AI112787.

AUTHOR CONTRIBUTIONS

Conceptualization and Methodology, S.S. and D.L.B.; Investigation, S.S., N.E.L., K.D.K., D.E.D., S.N., F.G., J.D.F., NIAID/DIR TBIP and L.E.V.; Resources, S.O., C.S.L., A.S., G.J.F., and C.E.B.; Original Draft, S.S. and D.L.B.; Writing—Review & Editing, S.S., K.D.K., S.N., F.G., C. S.L., A.S., G.J.F., L.E.V., C.E.B., and D.L.B.; Visualization, S.S., S.N., F.G., and J.D.F.; Supervision, D.L.B., A.S., L.E.V., and C.E.B.; Funding Acquisition, D.L.B., A.S., G.J.F., L.E.V., and C.E.B.

COMPETING INTERESTS

D.L.B. has patents on the PD-1/PD-1 pathway. G.J.F. has patents/pending royalties on the PD-1/PD-L1 pathway from Roche, Merck MSD, Bristol-Myers-Squibb, Merck KGA, Boehringer-Ingelheim, AstraZeneca, Dako, Leica, Mayo Clinic, and Novartis. G.J.F. has served on advisory boards for Roche, Bristol-Myers-Squibb, Xios, Origimed, Triursus, iTeos, NextPoint, IgM, Jubilant and GV20. G.J.F. has equity in Nextpoint, Triursus, Xios, iTeos, IgM, GV20, and Geode.

ADDITIONAL INFORMATION

Supplementary information The online version contains supplementary material available at https://doi.org/10.1038/s41385-021-00425-3.

Correspondence and requests for materials should be addressed to D.L.B.

Reprints and permission information is available at http://www.nature.com/reprints

Publisher's note Springer Nature remains neutral with regard to jurisdictional claims in published maps and institutional affiliations.

TUBERCULOSIS IMAGING PROGRAM

Janard L. Bleach[4], Ashley L. Butler[4], Emmuanual K. Dayao[4], Joel D. Fleegle[4], Felipe Gomez[4], Michaela K. Piazza[4], Katelyn M. Repoli[4], Becky Y. Slone[4], Michelle K. Sutphin[4], Alexandra M. Vatthauer[4], Laura E. Via[2,4,5], April M. Walker[4], Danielle M. Weiner[4] and Michael J. Woodcock[4]